Organic & Biomolecular Chemistry

Cite this: *Org. Biomol. Chem.*, 2011, **9**, 5720

www.rsc.org/obc

PAPER

Chemically engineered papain as artificial formate dehydrogenase for NAD(P)H regeneration†

Pierre Haquette,[a,b] Barisa Talbi,[a,b] Laure Barilleau,[a,b] Nathalie Madern,[a,b] Céline Fosse[c] and Michèle Salmain*[a,b]

Received 28th March 2011, Accepted 11th May 2011
DOI: 10.1039/c1ob05482a

Organometallic complexes of the general formula $[(\eta^6\text{-arene})Ru(N^\wedge N)Cl]^+$ and $[(\eta^5\text{-Cp*})Rh(N^\wedge N)Cl]^+$ where N^N is a 2,2′-dipyridylamine (DPA) derivative carrying a thiol-targeted maleimide group, 2,2′-bispyridyl (bpy), 1,10-phenanthroline (phen) or ethylenediamine (en) and arene is benzene, 2-chloro-*N*-[2-(phenyl)ethyl]acetamide or *p*-cymene were identified as catalysts for the stereoselective reduction of the enzyme cofactors $NAD(P)^+$ into NAD(P)H with formate as a hydride donor. A thorough comparison of their effectiveness towards NAD^+ (expressed as TOF) revealed that the Rh^{III} complexes were much more potent catalysts than the Ru^{II} complexes. Within the Ru^{II} complex series, both the N^N and arene ligands forming the coordination sphere had a noticeable influence on the activity of the complexes. Covalent anchoring of the maleimide-functionalized Ru^{II} and Rh^{III} complexes to the cysteine endoproteinase papain yielded hybrid metalloproteins, some of them displaying formate dehydrogenase activity with potentially interesting kinetic parameters.

Introduction

Numerous enzymes involved in important biocatalytic processes require the presence of low molecular weight species called cofactors that are essential for their catalytic activity. For instance, dehydrogenases that catalyze the reduction of carbonyl compounds to alcohols require nicotinamide adenine dinucleotide (NAD) or nicotinamide adenine dinucleotide phosphate (NADP) as cofactors which provide 2 e^- and 1 H^+ to the substrate.[1] Regeneration of these expensive cofactors is an important issue since they act as stoichiometric reagents. At the industrial level, coenzyme regeneration is achieved by using whole-cell biocatalysts or by addition of a sacrificial substrate (substrate-coupled reaction systems) or preferably a second enzyme that catalyses the transformation of $NAD(P)^+$ to NAD(P)H (enzyme-coupled reaction systems). Formate dehydrogenase (FDH) is the most widely used enzyme for NADH regeneration; it operates by catalysis of oxidation of formate to CO_2.[2]

In parallel, there have been several successful attempts to set up non-enzymatic NAD(P)H regeneration systems.[3] The most attractive systems make use of organometallic catalysts, essentially rhodium(III) complexes or, to a lesser extent, ruthenium(II) complexes. The first example of nicotinamide cofactor regeneration by organometallic catalysis was reported by Whitesides in 1982.[4] The system involved reduction of lactate to pyruvate by dihydrogen catalyzed by a diphosphine Rh^I complex. Pyruvate was then oxidized by the NAD-dependent enzyme lactate dehydrogenase with simultaneous formation of NADH. This cofactor was then used by horse liver alcohol dehydrogenase for the reduction of carbonyl compounds. Even if this regeneration system was indirect, it paved the way to combined organometallic/enzymatic catalyst systems for enantioselective synthesis.

A more versatile nicotinamide regeneration system was proposed by Steckhan *et al.* Regio-specific reduction of $NAD(P)^+$ to 1,4-NAD(P)H was achieved in homogeneous phase using sodium formate as the hydride source and $(Cp^*)(N^\wedge N)Rh^{III}$ catalysts where Cp* is $\eta^5\text{-}C_5Me_5$ and N^N is 2,2′-bipyridyl (bpy), 4,4′-Me_2bpy or 6,6′-Me_2bpy.[5–7] Fish *et al.* later reported that $[Cp^*Rh^{III}(bpy)(H_2O)]^{2+}$ was also able to catalyze the reduction of various NAD^+ models using formate as the hydride donor[8] and proposed the following catalytic cycle to fit the kinetics data (Scheme 1). Reaction of the aqua complex with formate gives the formato complex that decomposes to the hydrido complex by a β-elimination process releasing CO_2. The hydride is transferred regiospecifically to NAD^+ by a concerted mechanism facilitated by coordination of the amide functionality of the nicotinamide entity. Recycling of the aqua complex eventually occurs *via* displacement of the 1,4-dihydro product.

Alternatively, regeneration of NADH was achieved by an indirect electrochemical process using Cp*Rh(bpy) species as a

[a]*Chimie ParisTech, Laboratoire Charles Friedel, Paris, 75005, France. E-mail: Michele-salmain@chimie-paristech.fr; Fax: +33 143260061; Tel: +33 144276732*
[b]*CNRS, UMR 7223, Paris, 75005, France*
[c]*Chimie ParisTech, Laboratoire de spectrométrie de masse, Paris, 75005, France*

† Electronic supplementary Information (ESI) available: ESI-MS spectra of PAP-**4a** and PAP-**4b**. See DOI: 10.1039/c1ob05482a

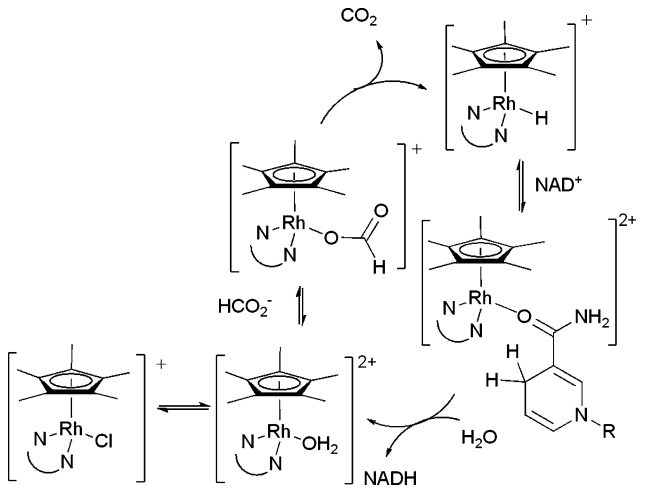

Scheme 1 Simplified mechanism of NAD(P)$^+$ reduction catalyzed by an Rh^{III} complex in the presence of formate as the hydride donor.[8]

mediator. The reduction of [Cp*Rh^{III}(bpy)] to Rh^I species allows the simultaneous transfer of 2 e^- and 1 H^+ to NAD(P)$^+$.[7,9–17] NADPH direct regeneration using H_2 as the reducing agent catalyzed by $[RuCl_2(TPPTS)_2]_2$ was proposed by Hembre in 2003.[18] Recently, phosphite was found as an alternative source of reducing equivalents for the Rh-catalyzed regeneration of NAD(P)H and $FADH_2$.[19]

The ability of the [Cp*Rh^{III}(bpy)(H_2O)]$^{2+}$ system to regenerate nicotinamide and flavin coenzymes[10,20,21] together with metal porphyrin derivatives[21–23] was exploited in various biosynthetical processes such as enantioselective reduction of prochiral ketones by alcohol dehydrogenases,[24–26] halogenation of tryptophane with tryptophane 7-halogenase,[27] epoxidation of styrene derivatives,[20] regioselective hydroxylation of 2-hydroxybiphenyl[28] and oxidation of organic sulfides[21,29] and camphor[30] by various monooxygenases.

We recently reported the synthesis of 2,2′-dipyridylamine (DPA) ligands functionalized by a maleimide group **1a** and **1b** (Scheme 2). These ligands were designed to enable covalent anchoring of derived catalytically active metal complexes to cysteine-containing proteins thanks to the presence of the maleimide group. Reaction of these ligands with [(η^6-arene)$Ru^{II}Cl_2]_2$ (arene = benzene or *p*-cymene) yielded the monomeric cationic complexes [(η^6-arene)Ru^{II}(**1a–b**)Cl]Cl **2a–b** (arene = benzene) and **3a–b** (arene = *p*-cymene) and these complexes were site-specifically anchored to the cysteine endoproteinase papain.[31] One of the structural features of papain, *i.e.* the presence of a single reactive cysteine residue within the enzyme active site, makes it a convenient model to construct artificial metalloenzymes.[32–36] By analogy with previously reported results on related Ru^{II} compounds,[26,37] we thought that these complexes may also catalyze the reduction of NAD^+ using formate as a hydride source. In this paper, we report the synthesis of Cp*Rh^{III} complexes **4a–b** including ligands **1a–b** and their ability, together with that of the previously described Ru^{II} complexes, to catalyze the reduction of NAD^+. Moreover, we also report the covalent anchoring of these Ru^{II}/Rh^{III} complexes to papain and show that some of the resulting artificial metalloenzymes acquire formate dehydrogenase activity.

Experimental

Materials and reagents

Solvents were dried and distilled by standard procedures and the syntheses were performed under an inert atmosphere of argon using standard Schlenk and vacuum-line techniques. NMR spectra were recorded on a 300 MHz Avance spectrometer (Bruker). High resolution mass spectra were recorded on a MStation JMS 700 (Jeol). UV-visible spectra were recorded on uv/mc2 spectrophotometer (Safas). Fluorescence measurements were carried out in a 1 cm pathlength quartz cell on an F-6200 spectrofluorimeter (Jasco). The excitation and emission slit widths were set at 5 nm. The scan speed was set to 125 nm min^{-1} with a data pitch of 1 nm. For the single wavelength kinetic measurements, the response was set to 0.5 s and data pitch to 1 s. Alternatively, fluorescence kinetic measurements were carried out on a microplate reader (BMG Labtech) with excitation and emission filters set to 340 and 470 nm, respectively. Ligands **1a–b** and complexes **2a–b** and **3a–b** were prepared according to our published procedure.[31] Complexes **5** and **6** were synthesized according to ref. 38. Complexes **7** and **8** were synthesized according to the literature.[39,40] [Cp*RhCl(μ-Cl)]$_2$ was prepared according to the literature procedure.[41] Papain (PAP^F) was purchased from Fluka (reference 76220) and purified by affinity chromatography according to a published procedure to

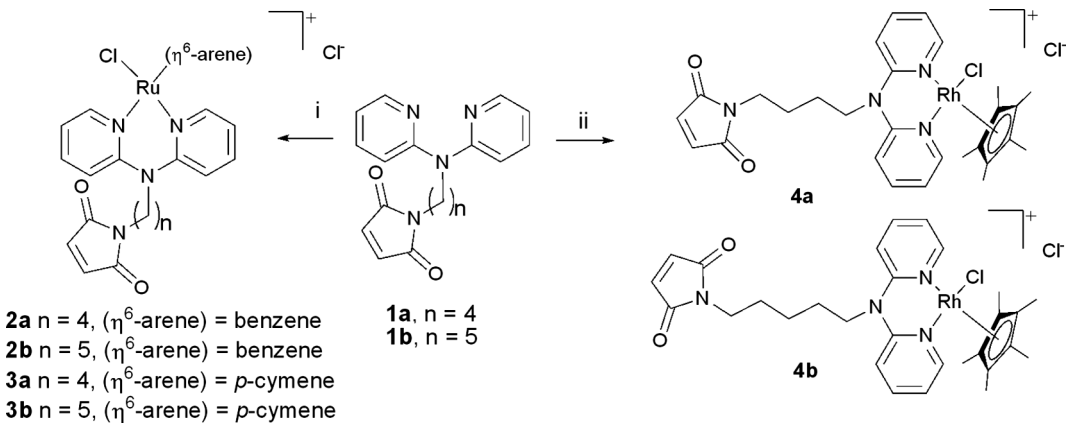

Scheme 2 Conditions: i: 0.5 [arene-RuCl(μ-Cl)]$_2$, CH_2Cl_2, RT, 16 h; ii: 0.5 [Cp*RhCl(μ-Cl)]$_2$, CH_2Cl_2, RT, 3 h.

yield PAP.[42] The hydrolytic activity of papain was measured with L-pyroglutamyl-L-phenylalanyl-L-leucine-*p*-nitroanilide (Bachem) as chromophoric substrate.[43]

Synthesis of the Rh^{III} complexes

$[Cp^*RhCl(\mu\text{-}Cl)]_2$ (50 mg, 0.08 mmol) was introduced into a Schlenk tube followed by CH_2Cl_2 (16 ml) and **1a** or **1b** (0.16 mmol). The mixture was stirred at room temperature for 3 h. The solvent was evaporated under reduced pressure and the residue was washed 3 times with 10 ml of diethyl ether. The orange solid was dried under vacuum.

[Cp*Rh(**1a**)Cl]Cl (**4a**): Yield 95%. ^{1}H NMR (D_2O, 300 MHz) δ 8.50 (dd, 2H, J = 5.7 Hz, J = 1.2 Hz), 7.99 (t, 2H, J = 7.9 Hz), 7.42 (d, 2H, J = 8.4 Hz), 7.32 (t, 2H, J = 6.3 Hz), 6.81 (s, 2H), 4.04–3.96 (m, 2H), 3.55 (t, 2H, J = 6.8 Hz), 1.75–1.50 (m, 4H), 1.48 (s, 15H). ^{13}C NMR (D_2O, 75 MHz) δ 173.2, 155.4, 152.0, 141.4, 134.3, 122.0, 116.8, 97.3, 49.6, 37.0, 25.3, 24.5, 8.1. HRMS calcd for $C_{28}H_{33}ClN_4O_2Rh^+$ 595.13471, found 595.13530.

[Cp*Rh(**1b**)Cl]Cl (**4b**): Yield 95%. ^{1}H NMR (D_2O, 300 MHz) δ 8.52 (dd, 2H, J = 5.7 Hz, J = 1.2 Hz), 8.00 (t, 2H, J = 7.9 Hz), 7.43 (d, 2H, J = 8.4 Hz), 7.33 (t, 2H, J = 6.3 Hz), 6.82 (s, 2H), 4.05–3.95 (m, 2H), 3.52 (t, 2H, J = 6.8 Hz), 1.80–1.35 (m, 6H), 1.52 (s, 15H). ^{13}C NMR (D_2O, 75 MHz) δ 173.3, 155.4, 151.8, 141.3, 134.3, 121.8, 116.8, 97.3, 50.1, 37.1, 27.0, 26.2, 23.3, 8.1. HRMS calcd for $C_{29}H_{35}ClN_4O_2Rh_+$ 609.15036, found 609.13116.

Conjugation of 3a to PAP^F

PAP^F (50 mg) was dissolved in 20 mM phosphate buffer, 0.4 M NaCl, pH 7 (5 ml). Complex **3a** (5 eq.) was added to the solution and the mixture was incubated for 15 h at r.t. The solution was then dialyzed in water for 40 h at 4 °C. The protein concentration was calculated from absorbance measurement at 280 nm taking $A_{280}(1\%) = 20.0$ for PAP^F[44] and $\varepsilon_{280} = 8700$ for **3a**.

Conjugation of 4a–b to PAP

Affinity-purified papain (7.5 μM in 20 mM phosphate 0.4 M NaCl, pH 7; 10 ml) was mixed with **4a** or **4b** (1 mM in DMSO, 0.75 ml, 10 eq.) and solutions were incubated overnight at room temperature without stirring. The absence of hydrolytic activity of the solutions on PFLNa was checked and they were then submitted to gel filtration chromatography (Hiprep 26/10 desalting, GE Healthcare) using 0.15 M NaCl as eluent at 5 ml min^{-1} to remove excess reagent. The conjugate solutions were concentrated to 2 ml by ultrafiltration in a 50 ml stirred cell equipped with a 5kD Ultracell membrane (Millipore). The protein concentration was calculated from absorbance measurement at 280 nm taking ε_{280} = 57 600 for papain and ε_{280} = 5500 for **4a–b**. A fraction of these solutions (0.5 ml) was dialyzed in water to remove NaCl and further concentrated to 50 μl with a centrifugal filter (Amicon ultra-0.5 5kD) to get suitable samples for ESI-MS analysis. ESI-MS: PAP-**4a**: 24 030 ± 2 [M − Cl + HCOO]; PAP-**4b**: 24 044 ± 6 [M − Cl + HCOO].

Conjugation of 4b to PAP^F

PAP^F (50 mg) was dissolved in 20 mM phosphate, 0.4 M NaCl pH 7 (9 ml). Complex **4b** (1 ml of 1 mM solution in DMSO, 1.6 molar eq.) was added to the solution and the mixture was incubated for 24 h at r.t. A solution of *N*-ethylmaleimide (0.1 M; 100 μl, 1 mM final concentration) was added and after another 30 min, the protein was separated from excess reagents by gel filtration (Hiprep 26/10, GE Healthcare) using 0.15 M NaCl at 5 ml min^{-1} as eluent. The conjugate solution was concentrated to 1.2 ml by ultrafiltration in a 50 ml stirred cell (Millipore) equipped with an Ultracell 5kD membrane (Millipore). The resulting yellow solution was eventually dialyzed in water for 24 h at 4 °C.

Conjugation of 5 to PAP^F

PAP^F (100 mg) was dissolved in 20 mM phosphate, 0.4 M NaCl pH 7 (10 ml). Complex **5** (3.5 mg, 0.66 mM final concentration, 5 molar eq.) was added to the solution and the mixture incubated overnight at r.t. A solution of *N*-ethylmaleimide (0.1 M; 100 μl, 1 mM final concentration) was added and after another 30 min, the solution was filtered on a 0.22 mm filter. The protein was separated from excess reagents by gel filtration (Hiprep 26/10, GE Healthcare) using 0.15 M NaCl at 2 ml min^{-1} as eluent. The conjugate solution was concentrated to 2.3 ml by ultrafiltration in a 50 ml stirred cell (Millipore) equipped with an Ultracell 5kD membrane (Millipore). The resulting brown solution was eventually dialyzed in water for 40 h at 4 °C and kept at –20 °C until use. The protein concentration was calculated from absorbance measurements at 280 nm taking ε_{280} = 18 200 for **5**.

Conjugation of 6 to PAP^F

The same procedure was applied for the conjugation of **6** except that reaction was carried out in water with pH adjusted to 7 by addition of 0.1 M NaOH and the NEM step was omitted. The protein concentration was calculated from absorbance measurement at 280 nm taking ε_{280} = 8800 for **6**.

Catalysis of NAD^+ reduction by the ruthenium complexes and their metalloenzymes

An aqueous solution of NAD (50 mM, 320 μl, final concentration 8 mM) was mixed with a solution of sodium formate (3.5 M, 200 μl, final concentration 350 mM) and 0.1 M phosphate buffer pH 7 (1480 μl). This mixture was transferred into a 1 cm pathlength quartz cuvette and equilibrated at 45 or 50 °C. After 5 min, a volume of Ru catalyst solution (in DMSO for the complexes or in water for the metalloenzymes) was added to reach a final concentration of 0.16 mM. Formation of NADH was monitored by repeated measurements of the emission spectrum between 350 and 550 nm (λ_{ex} = 340 nm) over a period of 30 to 120 min. The peak height at 473 nm was measured on each spectrum and calibrated against solutions of NADH at known concentrations in the same medium at the same temperature (without catalyst).

Catalysis of NAD^+ reduction by the rhodium complexes and their metalloenzymes

The same procedure was applied with the rhodium complexes and the corresponding metalloenzymes except that the final concentration of catalyst was set to 2 or 1.2 μM and the formation of NADH was monitored by single wavelength fluorescence measurements over a period of 5–10 min. Alternatively, monitoring of NADH

formation was carried out in black 96-well microtiter plates (Nunc) with reagent volumes divided by 10 (total volume = 200 µl).

Results and discussion

Synthesis

Ligands **1a–b** and the Ru^{II} complexes **2a–b** and **3a–b** were synthesized according to our previously described method.[31] The monocationic Rh^{III} complexes **4a–b** were obtained in nearly quantitative yield as orange powders by reaction of ligands **1a–b** with the dimer $[Cp^*RhCl(\mu\text{-}Cl)]_2$ in dichloromethane at room temperature (Scheme 2). The complexes were characterized by ^1H and ^{13}C NMR. After complexation by rhodium, the protons of the DPA ligands were shifted downfield and a singlet at 1.66 ppm was observed for the 15 protons of the Cp* ligand.

The Ru and Rh complexes are soluble in water and, as they possess a Cl^- leaving group, we expected that they could undergo hydrolysis in water according to Scheme 3. Such a behaviour was previously observed for related complexes and the aquation of the chloro complexes and anation of the aqua complexes could be monitored by spectrophotometry.[45]

$$\begin{cases} [(\eta^6\text{-arene})Ru(N\text{^}N)Cl]^+ \\ [(\eta^5\text{-}Cp^*)Rh(N\text{^}N)Cl]^+ \end{cases} \underset{Cl^-}{\overset{H_2O}{\rightleftharpoons}} \begin{cases} [(\eta^6\text{-arene})Ru(N\text{^}N)(H_2O)]^{2+} \\ [(\eta^5\text{-}Cp^*)Rh(N\text{^}N)(H_2O)]^{2+} \end{cases}$$

Scheme 3 Aquation/anation reactions.

The largest change in absorption was observed at 280 and 270 nm for **3b** and **4a**, respectively. These wavelengths were selected for the kinetic studies of aquation and anation. Fig. 1 depicts the change of absorbance at 270 nm occurring during the hydrolysis of **4a**. The time-dependence of the absorbance followed a first-order kinetics and yielded the first-order rate constants k_{H_2O} (Table 1).

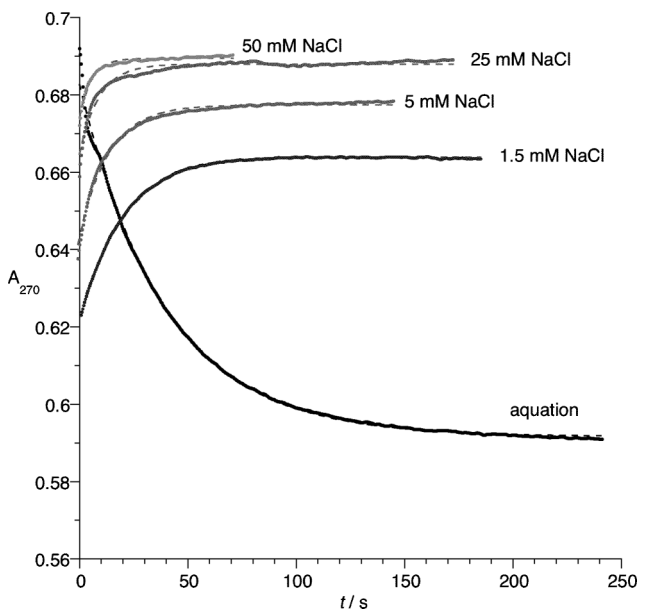

Fig. 1 Time-dependence of the absorbance at 270 nm during the hydrolysis of **4a** (0.1 mM) at RT. The dotted lines represent computer fits giving the first order rate constant for aquation and the pseudo-first order rate constants for anation reactions.

Table 1 Rates and equilibrium constants for the hydrolysis of the Ru^{II} and Rh^{III} complexes[a]

Complex	$k_{H_2O}/10^{-3}$ s^{-1}	$k_{Cl}/10^{-3}$ M^{-1} s^{-1}	$K/10^{-3}$ M
3b	0.0256	0.34	75
4a	25	2570	9.7
5	0.147	43	3.5
6	0.192	82	2.3
7	0.182	41	4.5
8	1.83	440	8.8

[a] [complex] = 0.1 mM, T = 20 °C.

The reverse anation reactions were studied by adding NaCl in excess to solutions of **3b** and **4a** having reached equilibrium. The second order rate constants k_{Cl} were calculated from the slope of the plots of the pseudo first order rate constants k'_{Cl} *versus* $[Cl^-]$ (Table 1). The values of the equilibrium constants K were calculated from the ratios of k_{H_2O}/k_{Cl} (Table 1).

For comparison, the kinetics of hydrolysis of the related Ru^{II} complexes **5**, **6**, **7** and **8** depicted in Fig. 2 was studied under similar conditions.

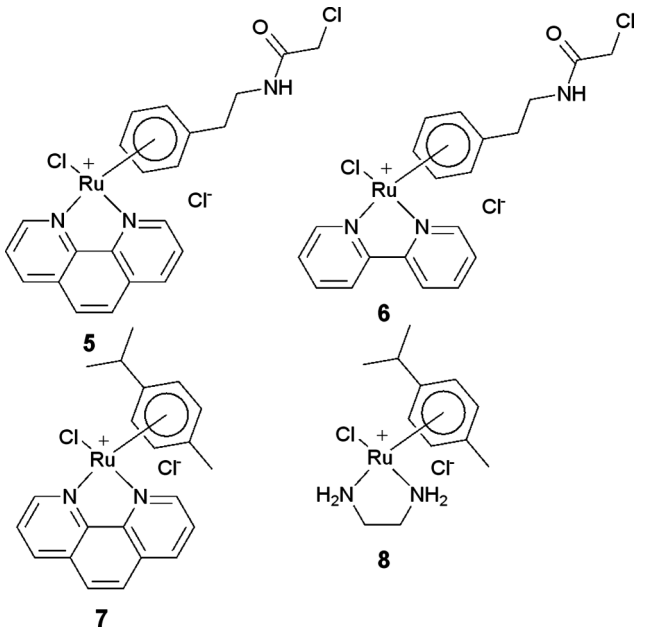

Fig. 2 Structures of other Ru^{II} complexes.

At first sight, the Rh^{III} complex **4a** hydrolyzed much faster than all the Ru^{II} complexes under study (from 14 to 100 times faster). The rate of the reverse anation reaction was also larger for the Rh^{III} complex (6 to 8000 times). Among the Ru^{II} complexes we noticed a clear influence of the N^N ligand on the hydrolysis rate. Compounds **3b**, **7** and **8** that only differ by the N^N ligand, displayed very different hydrolysis rates, with **8** hydrolyzing 10 times faster than **7** and 70 times faster than **3b**. This difference is probably related to electronic effects. The nature of the arene ligand also influenced the rate of hydrolysis but to a lesser extent, as illustrated by the difference of rates for **5** and **7**. Interestingly, no significant change of the UV spectrum of an aqueous solution of **2a** (or **2b**) was noticed over time, indicating that hydrolysis was too slow to measure for these complexes.

Table 2 Reduction of NAD^+ using formate as the hydride source in the presence of various catalysts[a]

Entry	Catalyst	pH	TOF[b]	Relative TOF[c]
1	**2b**	7	0.0056	0.3
2	**3a**	7	0.0053	0.3
3	**3b**	7	0.0055	0.3
4	**4a**	7	85.5	4750
5	**4b**	7	71	3940
6	**5**	5	0.016	0.9
7	**5**	6	0.023	1.3
8	**5**	7	0.018	1
9[d]	**5**	7	0.015	0.8
10[e]	**5**	7	0.048	2.7
11	**6**	7	0.098	5.4
12	**7**	7	0.072	4
13	**8**	7	0.109	6
14[f]	$[Cp^*Rh(bpy)(H_2O)]^{2+}$	7	81.5	4280
15	PAP^F-**3a**	7	0	0
16[g]	PAP-**4a**	7	52.1	2900
17[g]	PAP-**4b**	7	42.5	2360
18[e]	PAP^F-**5**	7	0.031	0.17
19	PAP^F-**6**	7	0.01	0.55
20	PAP^F-**4b**	7	20.2	1120

[a] Conditions: [NAD^+] = 8 mM, [HCOONa] = 350 mM, 0.1 M phosphate buffer, v = 2 ml, [Ru] = 160 μM or [Rh] = 2 μM, T = 45 °C; [b] Turnover frequency defined as mol product/mol catalyst/h; [c] Calculated relatively to the TOF of compound **5** arbitrarily set to 1 (entry 8); [d] T = 40 °C; [e] T = 50 °C; [f] Ref. 5 Conditions: [NAD^+] = 0.42 mM, [HCOONa] = 500 mM, [Rh] = 25 μM, 0.1 M phosphate pH 7, v = 1.5 ml, T = 38 °C; [g] [Rh] = 1.2 μM.

Catalytic reduction of NAD^+ by the complexes

As mentioned in the introduction, several Ru and Rh complexes have previously been shown to catalyze the regioselective reduction of NAD^+ to 1,4-NADH using formate as a hydride source. We carried out the same kind of experiment with complexes **2–8** under standard conditions. The formation of NADH was monitored continuously by spectrofluorimetry at 473 nm (λ_{ex} = 340 nm) taking advantage of the fact that NADH is fluorescent whereas NAD is not. At the beginning of the conversion, the intensity of fluorescence varied linearly over time. The turnover frequency (TOF), defined as the quantity of NADH formed per unit of time divided by the quantity of catalyst, was deduced from these kinetic measurements and standard curves of NADH established under the same experimental conditions (Table 2). At this stage, no characterisation of the final reduction product was performed and we inferred that only the kinetic 1,4-dihydro isomer was formed.

The first striking observation retrieved from this set of data is that the Rh^{III} complexes were tremendously more active than the Ru^{II} complexes. The TOF for compound **4b** was *ca.* 13 000 times higher than that of the analogous Ru^{II} complex **3b** (entries 5 and 3). Such a difference of reactivity had been previously noticed from a comparison of the catalytic activities of a series of Ru^{II}, Rh^{III} and Ir^{III} complexes comprising various N^N ligands.[26]

The TOF measured for the rhodium complexes were all in the same order of magnitude as that determined for the prototypical complex $[Cp^*Rh(bpy)(H_2O)]^{2+}$ (entry 14).[5,7] Similarly, $Cp^*Rh^{III}(L_2)$ complexes are generally much more active catalysts in the transfer hydrogenation of ketones than the analogous $(arene)Ru^{II}(L_2)$ complexes.[46–48] Among the set of Ru^{II} complexes with an unsubstituted or a mono-substituted arene ligand (complexes **2b**, **5** and **6**), we noticed a significant influence of the N^N ligand on the catalytic efficiency of the complexes (entries 1, 8 and 11) yielding the following order bpy > phen > DPA. The Ru^{II} complexes with the same *p*-cymene ligand but with a different N^N ligand, *i.e.* complexes **3a–b**, **7** and **8**, also displayed different activities (entries 2, 3, 12 and 13) yielding the following order en > phen > DPA. In the Ru(DPA) complex series (**2a–b** and **3a–b**), there was no substantial effect of the arene ligand on the TOF (entries 1–3). Conversely, in the Ru(phen) complex series (**5** and **7**), replacement of the mono-substituted arene by *p*-cymene led to an increase of the TOF by a factor of 4 (entries 8 and 12). Such an effect of the arene ligand on the catalytic activity of Ru^{II} complexes has been previously attributed to the higher donor character of the substituted arene.[37]

Somehow, the catalytic efficiency was related to the rate of hydrolysis of the complexes, as the most efficient catalysts were also the species with the most labile chloride ligand. It is in agreement with the catalytic cycle depicted in Scheme 1.

We next studied the influence of pH on the activity of complex **5** (Table 1, entries 6–8). The largest TOF was measured at pH 6.0. It was also noticed that the catalytic activity of **5** increased with the temperature (entries 8–10), as previously noticed in the literature.[7,19,20,26] Next, the catalytic efficiency of **4a** towards the reduction of NAD^+ was investigated as a function of formate concentration and a Michaelis-type (saturation) kinetic behaviour was observed (Fig. 3), as previously reported in the literature.[5,8,37]

This behaviour was explained by the occurrence of a pre-equilibium between the aqua and the formato complexes and the formation of the hydrido complex as the rate-determining step (Scheme 1). Non linear regression analysis of the data set according to the Michaelis–Menten equation gave a K_m(formate) of 250 ± 25 mM and a maximum TOF (TOF_{max}) of 34.7 ± 1.3 h^{-1}. The Michaelis constant was slightly higher than those determined for $[Cp^*Rh(bpy)(H_2O)]^{2+}$ (140 mM) and $[(hmb)Ru(en)Cl]^+$ (58 mM) (hmb = hexamethylbenzene).

The same experiment was repeated with a fixed concentration of formate and a variable concentration of substrate. Again a Michaelis-type (saturation) kinetic behaviour was observed (Fig. 3). Non linear regression analysis of the data set according to the Michaelis–Menten equation gave a K_m(NAD) of 27.1 ± 2.5 μM and a TOF_{max} of 43.5 ± 0.7 h^{-1}. This is in accordance with a "coordination pre-equilibrium" stage during which NAD^+ coordinates to the metal center *via* the carbonyl of its amide function before hydride transfer takes place.[8,10]

Catalytic reduction of $NAD(P)^+$ by the metallopapains

Although Cp*Rh(bpy) is recognized as a very efficient catalyst for chemical regeneration of NAD(P)H, it presents a serious drawback when associated with NAD(P)-dependent enzymes. Indeed, a mutual inactivation of the metal catalyst and the biocatalyst was seen to occur during the biocatalytic process.[16,26,28,30] A systematic investigation showed that, because the metal complex possesses a free coordination site, essential residues of the biocatalyst can coordinate to the complex and hence impair its enzymatic activity.[49] Several strategies have been proposed to obviate this issue, such as the use of a nucleophilic buffer to saturate the

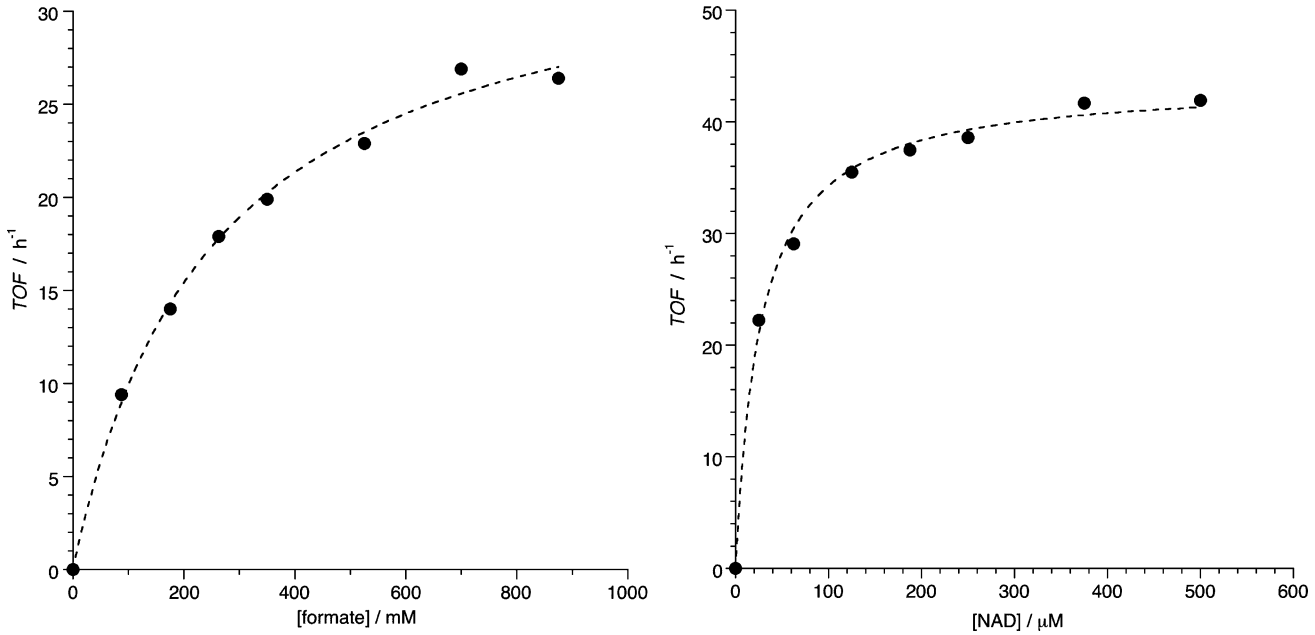

Fig. 3 Left: TOF vs. [formate]. Conditions: [**4a**] = 2 μM, [NAD] = 8 mM, T = 38 °C, 0.1 M phosphate pH 7. Right: TOF vs. [NAD]. Conditions: [**4a**] = 2 μM, [formate] = 700 mM, T = 38 °C, 0.1 M phosphate pH 7.

coordination sites[49] or the addition of a non reactive protein in the reactional medium.[15]

We hypothesized that anchoring of the Ru^{II}/Rh^{III} catalysts to a protein in a controlled, site-selective fashion may yield a more stable and efficient catalyst for NADH regeneration in the presence of other enzymes. Besides, Steckhan and *et al.* emphasized the advantages of macromolecular, yet soluble, Rh catalysts for NADH regeneration.[6]

To this purpose, complexes **3a**, **4a–b**, **5** and **6** were conjugated to papain from *Carica papaya* (either in its raw form, PAP^F, or in its affinity-purified form, PAP). This enzyme is a member of the cysteine endoproteinase family; it catalyzes the hydrolysis of peptides/proteins and also displays some esterase activity.[50] Several interesting structural features of papain prompted us and other authors to select this protein to construct artificial metalloproteins by covalent anchoring of metal complexes at its single free cysteine residue (Cys25).[32–36] Upon reaction with the complexes, we observed that papain completely lost its ability to catalyze the hydrolysis of peptide and ester chromogenic substrates. Furthermore, actual anchoring of the Rh^{III} metal complexes to papain was demonstrated by ESI-MS analysis of the modified protein (Fig. S1 and S2, ESI†). The molecular masses calculated from the multi-charged spectra were 13 amu higher than the molecular mass, resulting from the addition of papain and the complexes. This discrepancy was explained by the high lability of the chloride ligand in complexes **4a–b** (see above) and the high concentration of formic acid in the medium used for ESI-MS analysis that led to the generation of the formato species *in situ*.

The ability of the metallopapain species to catalyze the reduction of NAD^+ in the presence of formate was then investigated in the same experimental conditions taken for the isolated complexes. Again, characterization of the final reduction product was not attempted and we inferred it to be the 1,4-dihydro isomer. The metallopapain derived from **3a** displayed no measurable catalytic activity, while those derived from **5** and **6** displayed weak but measurable activities (TOF = 0.0031 and 0.01 h^{-1}, respectively). Noticeably, the catalytic activity of PAP^F-**5** and PAP^F-**6** was 6.4 and 10% of the activity of the isolated complexes, respectively (compare entries 9 and 18 and 11 and 19 in Table 2). Thus covalent linking of the Ru^{II} complexes to papain severely reduced or even completely abolished their ability to catalyze the reduction of NAD^+ in the presence of formate. Conversely, the metallopapain derivatives resulting from conjugation with **4a** and **4b** led to TOF of 51.2 and 42.5 h^{-1}, respectively (Table 2, entries 16 and 17). They were both active catalysts in the reduction of NAD under mild conditions.

Conjugation of the metal complexes to the protein only moderately affected their activity as a decrease of 40% of the TOF was noticed for the metalloenzymes with respect to the isolated complexes (compare entries 4 and 16 and 5 and 17 in Table 2). This decreased activity may be due to steric reasons, as the site of catalysis may be less accessible to the NAD substrate when the rhodium centre is anchored to papain.

The influence of formate and NAD concentration on the rate of formation of NADH in the presence of PAP-**4a** and PAP-**4b** was further examined (Fig. 4). As for the isolated complexes **4a–b**, the kinetics of reduction of NAD catalyzed by the metallopapains obeyed a Michaelis-type kinetic behaviour with K_m(NAD) and K_m(formate) in the same order of magnitude (Table 3). Again, incorporation of the metal cofactors into the papain scaffold moderately affected the kinetic parameters. The artificial formate dehydrogenases resulting from the anchoring of the rhodium complexes to papain were very stable since the reduction experiments were carried out within a period of one year and no change of the catalytic activity was observed during this period.

For comparison, the kinetic parameters of FDH from *Candida boidinii* and the artificial metalloenzymes are reported in Table 3.

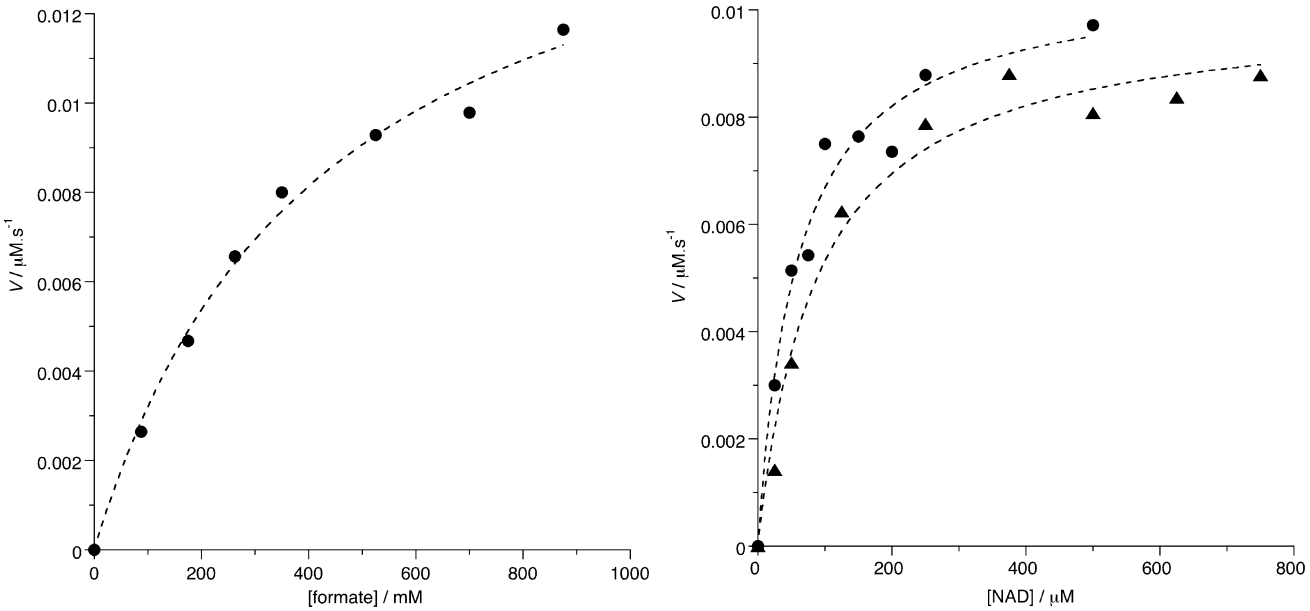

Fig. 4 Rate of formation of NADH as a function of [formate] (left) or [NAD] (right) catalyzed by PAP-**4a** (●) or PAP-**4b** (▲). Conditions: [PAP-**4a**] = 1.25 μM; [PAP-**4b**] = 1.2 μM; T = 38 °C, 0.1 M phosphate pH 7. Left: [NAD] = 8 mM. Right: [formate] = 700 mM.

Table 3 Kinetic parameters of PAP-Rh metalloenzymes and FDH from *Candida boidinii*

	PAP-**4a**	PAP-**4b**	PAP^F-**4b**	FDH
K_m(NAD) (μM)	59 ± 11[a]	89 ± 17[a]	n.d.	90[b]
K_m(formate) (mM)	425 ± 61[a]	n.d.	n.d.	13[a]
k_{cat}(NAD) (h^{-1})	30.5 ± 1.7[a]	30.0 ± 1.4[a]	n.d.	8400[d]
Spec. act. ($U.mg^{-1}$)	0.04	0.03[c]	0.013[c]	2.4[b]
Rel. act. to NADP (%)	n.d.	n.d.	60	0

[a] Conditions: *cf.* caption of Fig. 4. [b] Conditions: [NAD] = 8 mM; [formate] = 350 mM; T = 45 °C, 0.1 M phosphate pH 7. [c] Ref. 53; Conditions: [NAD] = 1.7 mM; [formate] = 170 mM, T = 30 °C, 50 mM phosphate pH 7.0. [d] Ref. 10

Table 4 Inhibition of PAP^F-**4b**[a]

Inhibitor	Concentration	Inhibition
Cl^-	10 mM	60%
	100 mM	93%
N_3^-	10 μM	6%
	100 μM	50%
	1000 μM	92%

[a] Conditions: [NAD] = 8 mM; [formate] = 350 mM; [PAP^F-**4b**] = 2 μM; T = 45 °C, 0.1 M phosphate pH 7

While K_m(NAD) was very close for all the enzymes, K_m(formate) was higher for the artificial metalloenzyme PAP-**4a** and the specific activity of all the metalloenzymes was lower than that of FDH. Interestingly, the artificial FDH resulting from covalent anchoring of **4b** to raw papain (PAP^F-**4b**) was less active than that obtained from affinity-purified papain. Raw papain (which is essentially dry papaya latex) is in fact composed of a mixture of 4 cysteine endoproteinases, among which papain only accounts for 8%.[51] Because of their close structure and reactivity, complex **4b** is expected to unselectively bind to all four enzymes, eventually leading to a different metalloenzyme in this case. Therefore, it indicates that the protein scaffold had a definite influence on the final formate hydrogenase activity.

PAP^F-**4b** was also able to catalyze the reduction of $NADP^+$ into NADPH, but with a 40% lower efficiency with respect to NAD^+. Most surprisingly, complex **4b** also displayed a 40% lower catalytically activity on $NADP^+$, so that this decreased efficiency was not due to the anchoring of the reactive species within the protein host. This finding was rather unexpected since other Rh^{III} complexes catalyzed the reduction of NAD and NADP with equal efficiency,[7] and the additional phosphate group in NADP is remote from the site of reaction. Nevertheless, PAP^F-**4b** was active on NADP, conversely to FDH which is specific to NAD.[52]

Finally, a study of the effect of chloride and azide on the catalytic activity of PAP^F-**4b** on NAD was carried out (Table 4). As expected, chloride anions behaved as an inhibitor of PAP^F-**4b**, most probably by competitive coordination to the metal center (see the anation experiment and the catalytic cycle in Scheme 1). Azide also behaved as an inhibitor of PAP^F-**4b**. It was an even stronger inhibitor than Cl^- (IC_{50} roughly equal to 100 μM), probably because it bound more tightly than chloride to Rh. It is interesting to note that azide is also a potent inhibitor of FDH (10 μM leads to 1% of activity)[53] thanks to its structural analogy with the product of reaction, CO_2.

Conclusions

A series of organometallic complexes of the general formula [(η^6-arene)Ru(N^N)Cl]$^+$ and [(η^5-Cp*)Rh(N^N)Cl]$^+$ were identified as catalysts for the reduction of the enzyme cofactors NAD(P)$^+$ to NAD(P)H, with formate as a hydride donor. Comparison of their catalytic efficiency towards NAD^+ (expressed as TOF) revealed that the Rh^{III} complexes were tremendously more potent than the Ru^{II} complexes. Within the Ru^{II} complex series, the

ligands forming the coordination sphere around the metal had a noticeable influence on the activity of the complexes. Covalent anchoring of the maleimide-functionalized complexes to the cysteine endoproteinase papain yielded hybrid metalloproteins, some of them displaying formate dehydrogenase activity. As the isolated complexes, the papain-Rh^{III} derivatives were the most potent metalloenzyme catalysts. The next step is now to combine the artificial formate dehydrogenase with NAD-dependent alcohol dehydrogenase to carry out asymmetric reduction of ketones. In parallel, other functional Rh^{III} complexes with different linker arms will be synthesized to try and improve the metalloenzymes catalytic activity.

Acknowledgements

The Centre National de la Recherche Scientifique (CNRS) and the French Ministry of Research are gratefully acknowledged for financial support.

Notes and references

1 W. A. Van Der Donk and H. Zhao, *Curr. Opin. Biotechnol.*, 2003, **14**, 421–426.
2 A. Berenguer-Murcia and R. Fernandez-Lafuente, *Curr. Org. Chem.*, 2010, **14**, 1000–1021.
3 R. Wichman and D. Vasic-Racki, *Adv. Biochem. Engin. Biotechnol.*, 2005, **92**, 225–260.
4 O. Abril and G. M. Whitesides, *J. Am. Chem. Soc.*, 1982, **104**, 1552–1554.
5 R. Ruppert, S. Herrmann and E. Steckhan, *J. Chem. Soc., Chem. Commun.*, 1988, 1150–1151.
6 E. Steckhan, S. Herrmann, R. Ruppert, J. Thömmes and C. Wandrey, *Angew. Chem., Int. Ed. Engl.*, 1990, **29**, 388–390.
7 E. Steckhan, S. Herrmann, R. Ruppert, E. Dietz, M. Frede and E. Spika, *Organometallics*, 1991, **10**, 1568–1577.
8 C. H. Lo, C. Leiva, O. Buriez, J. B. Kerr, M. M. Olmstead and R. H. Fish, *Inorg. Chem.*, 2001, **40**, 6705–6716.
9 R. Ruppert, S. Herrmann and E. Steckhan, *Tetrahedron Lett.*, 1987, **28**, 6583–6586.
10 F. Hollmann, B. Witholt and A. Schmid, *J. Mol. Catal. B: Enzym.*, 2003, **19–20**, 167–176.
11 K. Delecouls-Servat, A. Bergel and R. Basseguy, *Bioprocess Biosyst. Eng.*, 2004, **26**, 205–215.
12 K. Delecouls-Servat, R. Basseguy and A. Bergel, *Chem. Eng. Sci.*, 2002, **57**, 4633–4642.
13 F. Hildebrand, C. Kohlmann, A. Franz and S. Lutz, *Adv. Synth. Catal.*, 2008, **350**, 909–918.
14 K. Vuorilehto, S. Lutz and C. Wandrey, *Bioelectrochemistry*, 2004, **65**, 1–7.
15 F. Hildebrand and S. Lutz, *Tetrahedron: Asymmetry*, 2007, **18**, 1187–1193.
16 F. Hildebrand and S. Lutz, *Chem.–Eur. J.*, 2009, **15**, 4998–5001.
17 V. Höllrigl, K. Otto and A. Schmid, *Adv. Synth. Catal.*, 2007, **349**, 1337–1340.
18 P. S. Wagenknecht, J. M. Penney and R. T. Hembre, *Organometallics*, 2003, **22**, 1180–1182.
19 M. Mifsud Grau, M. Poizat, I. W. C. E. Arends and F. Hollmann, *Appl. Organomet. Chem.*, 2010, **24**, 380–385.
20 F. Hollmann, P.-C. Lin, B. Witholt and A. Schmid, *J. Am. Chem. Soc.*, 2003, **125**, 8209–8217.
21 F. Hollmann and A. Schmid, *J. Inorg. Biochem.*, 2009, **103**, 313–315.
22 P. A. Gosling and R. J. M. Nolte, *J. Mol. Catal. A: Chem.*, 1996, **113**, 257–267.
23 J. H. van Esch, M. A. M. Hoffmann and R. J. M. Nolte, *J. Org. Chem.*, 1995, **60**, 1599–1610.
24 D. Westerhausen, S. Herrmann, W. Hummel and E. Steckhan, *Angew. Chem., Int. Ed. Engl.*, 1992, **31**, 1529–1531.
25 C. H. Lo and R. H. Fish, *Angew. Chem., Int. Ed.*, 2002, **41**, 478–481.
26 J. Canivet, G. Suss-Fink and P. Stepnicka, *Eur. J. Inorg. Chem.*, 2007, 4736–4742.
27 S. Unversucht, F. Hollmann, A. Schmid and K. H. van Pee, *Adv. Synth. Catal.*, 2005, **347**, 1163–1167.
28 J. Lutz, F. Hollmann, T. V. Ho, A. Schnyder, R. H. Fish and A. Schmid, *J. Organomet. Chem.*, 2004, **689**, 4783–4790.
29 G. de Gonzalo, G. Ottolina, G. Carrea and M. W. Fraaije, *Chem. Commun.*, 2005, 3724–3726.
30 J. D. Ryan, R. H. Fish and D. S. Clark, *ChemBioChem*, 2008, **9**, 2579–2582.
31 P. Haquette, B. Dumat, B. Talbi, S. Arbabi, J.-L. Renaud, G. Jaouen and M. Salmain, *J. Organomet. Chem.*, 2009, **694**, 937–941.
32 L. Panella, J. Broos, J. Jin, M. W. Fraaije, D. B. Janssen, M. Jeromius-Stratingh, B. L. Feringa, A. J. Minnaard and J. G. de Vries, *Chem. Commun.*, 2005, 5656–5658.
33 M. T. Reetz, M. Rentzsch, A. Pletsch and M. Maywald, *Chimia*, 2002, **56**, 721–723.
34 M. T. Reetz, M. Rentzsch, A. Pletsch, M. Maywald, P. Maiwald, J. J.-P. Peyralans, A. Maichele, Y. Fu, N. Jiao, F. Hollmann, R. Mondière and A. Taglieber, *Tetrahedron*, 2007, **63**, 6404–6414.
35 B. Talbi, P. Haquette, A. Martel, F. de Montigny, C. Fosse, S. Cordier, T. Roisnel, G. Jaouen and M. Salmain, *Dalton Trans.*, 2010, **39**, 5605–5607.
36 P. Haquette, M. Salmain, K. Svedlung, A. Martel, B. Rudolf, J. Zakrzewski, S. Cordier, T. Roisnel, C. Fosse and G. Jaouen, *ChemBioChem*, 2007, **8**, 224–231.
37 Y. K. Yan, M. Melchart, A. Habtemariam, A. F. A. Peacock and P. J. Sadler, *JBIC, J. Biol. Inorg. Chem.*, 2006, **11**, 483–488.
38 P. Haquette, B. Talbi, S. Canaguier, S. Dagorne, C. Fosse, A. Martel, G. Jaouen and M. Salmain, *Tetrahedron Lett.*, 2008, **49**, 4670–4673.
39 J. Canivet, L. Karmazin-Brelot and G. Suss-Fink, *J. Organomet. Chem.*, 2005, **690**, 3202–3211.
40 R. E. Morris, R. E. Aird, P. del Socorro Murdoch, H. Chen, J. Cummings, N. D. Hughes, S. Parsons, A. Parkin, G. Boyd, D. I. Jodrell and P. J. Sadler, *J. Med. Chem.*, 2001, **44**, 3616–3621.
41 C. White, A. Yates, P. M. Maitlis and D. M. Heinekey, *Inorg. Synth.*, 1992, **29**, 228–234.
42 M. O. Funk, Y. Nakagawa, J. Skochdopole and E. T. Kaiser, *Int. J. Pept. Protein Res.*, 1979, **13**, 296–303.
43 I. Y. Filippova, E. N. Lysogorskaya, E. S. Oksenoit, G. N. Rudenskaya and V. M. Stepanov, *Anal. Biochem.*, 1984, **143**, 293–297.
44 D. J. Buttle, A. A. Kembhavi, S. L. Sharp, R. E. Shute, D. H. Rich and A. J. Barrett, *Biochem. J.*, 1989, **261**, 469–476.
45 F. Wang, H. Chen, S. Parsons, I. D. H. Oswald, J. E. Davidson and P. J. Sadler, *Chem.–Eur. J.*, 2003, **9**, 5810–5820.
46 Y. Himeda, N. Onozawa-Kamatsuzaki, H. Sugihara, H. Arakawa and K. Kasuga, *J. Mol. Catal. A: Chem.*, 2003, **195**, 95–100.
47 X. F. Wu, X. H. Li, A. Zanotti-Gerosa, A. Pettman, J. K. Liu, A. J. Mills and J. L. Xiao, *Chem.–Eur. J.*, 2008, **14**, 2209–2222.
48 N. A. Cortez, G. Aguirre, M. Parra-Hake and R. Somanathan, *Tetrahedron: Asymmetry*, 2008, **19**, 1304–1309.
49 M. Poizat, I. Arends and F. Hollmann, *J. Mol. Catal. B: Enzym.*, 2010, **63**, 149–156.
50 R. Arnon, *Methods Enzymol.*, 1970, **19**, 226–244.
51 M. Azarkan, A. El Moussaoui, D. van Wuytswinkel, G. Dehon and Y. Looze, *J. Chromatogr., B: Anal. Technol. Biomed. Life Sci.*, 2003, **790**, 229–238.
52 V. O. Popov and V. S. Lamzin, *Biochem. J.*, 1994, **301**, 625–643.
53 H. Schutte, J. Flossdorf, H. Sahm and M.-R. Kula, *Eur. J. Biochem.*, 1976, **62**, 151–160.